Carbon 108 (2016) 423–432

Contents lists available at ScienceDirect

Carbon

journal homepage: www.elsevier.com/locate/carbon

Systematic comparison of conventional and reductive single-walled carbon nanotube purifications

Adam J. Clancy, Edward R. White, Hui Huang Tay, Hin Chun Yau, Milo S.P. Shaffer*

Department of Chemistry, Imperial College London, South Kensington Campus, London, SW7 2AZ, UK

ARTICLE INFO

Article history:
Received 13 May 2016
Received in revised form
14 July 2016
Accepted 16 July 2016
Available online 18 July 2016

ABSTRACT

As-synthesised single-walled carbon nanotubes (SWCNTs) are often contaminated with amorphous carbon and residual catalyst particles. These contaminants have a detrimental effect on the effective mechanical and electronic properties, limiting their performance in many applications. A comparative series of SWCNT purifications including acid treatments, gas phase purifications and recently-developed reductive purifications have been conducted using a single commercial SWCNT type (Tuball™). Each of the purification procedures was selected for its potential scalability to bulk quantities and evaluated for the extent of impurity removal, SWCNT damage, and overall yield. Raman spectra confirmed that reductive purification using sodium naphthalide gave the lowest D/G ratio, suggesting that the sp^2 carbon framework was most effectively preserved, whilst removing a large proportion (~74%) of the metal impurities. Conversely, nitric acid treatment was most effective at removing virtually all the metal impurities, but the sp^2 carbon framework was most heavily damaged in the process. The development of scalable, one pot, reductive separations provides a useful new approach to SWCNT purification.

1. Introduction

Single-walled carbon nanotubes (SWCNTs) have superlative mechanical [1], (opto)electronic [2], and conductive properties and hence are promising materials in a huge array of diverse fields including nano-electronics [3], flexible transparent conductive films [4], composites [1], and drug delivery [5]. However, the impact of SWCNTs in the marketplace has been limited by both the high cost of the nanotubes and difficulties associated with processing of the as-produced materials. As-synthesised SWCNTs typically contain a variety of impurities, notably amorphous carbon and residual catalyst particles, usually encased in graphitic carbon shells or within the SWCNTs themselves. Many purification routes are known for SWCNTs and can be broadly categorised into acidic, gas phase, reductive (electro)chemical, and physical separation approaches. Due to the sheer number of variations and iterations, it would be impossible to summarise every purification strategy, but readers are directed to reviews [6,7] for a fuller understanding of possible approaches. Physical separation approaches typically employ selective adsorption, often in combination with size-exclusion chromatography [8] and/or density gradient ultracentrifugation [9]. While these approaches are invaluable for electronic/chirality/length separation, they are typically limited to very modest scales by the low yield and low concentration of individualised SWCNT dispersions produced by ultrasonication. This study focuses on methods for bulk purification to remove non-SWCNT components from mass-produced feedstock, using methods that are intrinsically scalable.

Simple acidic purifications dissolve exposed catalyst particles by heating and stirring of raw SWCNTs powder in acid [10], commonly HCl. However, as many catalyst particles are found within graphitic shells or the SWCNT interiors, the carbon must be etched, in order to access the metal and remove it more fully. Most commonly, oxidising acid [11], routinely HNO_3, is used to preferentially etch regions of high curvature (*i.e.* SWCNT caps and shells around catalysts), relying on their higher reactivity compared to the unstrained SWCNT sidewalls. However, the disruption of the carbon framework significantly reduces the mechanical and electronic properties of the SWCNTs [12]. Oxidative acid purification also introduces acidic debris and carboxylated carbonaceous impurities which must be removed separately [13], as also observed for graphene oxide [14].

A variety of other liquid phase competitive oxidation purification approaches are also known (*e.g.* $KMnO_4$, H_2SO_4/HNO_3) [15,16],

* Corresponding author.
E-mail address: m.shaffer@imperial.ac.uk (M.S.P. Shaffer).

http://dx.doi.org/10.1016/j.carbon.2016.07.034

but usually still cause extensive damage to the SWCNT structure as well as introducing additional impurities. Hydrogen peroxide provides an alternative, reacting with residual iron to form mildly oxidising hydroxyl radicals through Fenton chemistry [17]. These radicals can etch away the high curvature carbons in a less damaging manner than oxidising acids, allowing HCl, which is also present, to dissolve the newly exposed catalysts. While simple and relatively undamaging, this process was originally designed for HiPco SWCNTs (which contain high iron content, both exposed and encased) and has not been widely reported for other SWCNT types.

Gaseous purifications offer an alternative approach to oxidation of SWCNT samples, preferentially destroying amorphous carbons and high curvature sp^2 carbons through competitive combustion [10]. Encapsulated metal particles are exposed from both direct etching of their carbon shells and mechanical cracking of the shells as exposed metal expands on oxidation. Subsequent liquid phase (non-oxidative) acid washing is usually performed to remove the oxidised catalyst particles. The SWCNT structure is damaged when a strong gaseous oxidant (*e.g.* oxygen) is used, however milder oxidants, notably water vapour [18], can be employed to minimise SWCNT damage. With all gaseous purification approaches, the temperature and duration of heating can be varied to influence the balance between SWCNT damage and extent of purification.

Finally, recent developments have shown that reductive purifications can be performed through the (electro)chemical charging of SWCNTs and their impurities in aprotic, polar solvents, notably amides. True solutions of undamaged SWCNTs [19] form due to Columbic repulsion [20]; however, by limiting the extent of reduction, the impurities can be dissolved selectively [21]. Upon charging, small catalyst particles, amorphous carbons, and short (usually defective) SWCNTs diffuse into solution first, while the long SWCNTs must reptate out of the swollen bulk powder which requires significantly longer timescales [22]. Reductions can be carried out electrochemically [23], in liquid ammonia, or with sodium naphthalide (NaNp) in *N*,*N*-dimethylacetamide (DMAc) [22]. The extent of charging is controlled either by the electrochemical potential at which the SWCNTs are held, or the molar ratio of reducing agent to SWCNT carbons. In principle, if the charge is quenched carefully, the SWCNTs can be left undamaged by this process.

Annealing of SWCNTs at high temperature in inert atmosphere or *in vacuo* can be performed after purification to remove sp^3 defects/functional groups introduced during purification [7] to recover the SWCNT properties. However, routes which involve severe oxidation (or sonication) will introduce vacancy defects [24] and/or become shortened irreparably; in this case, annealing to remove surface functionality will only retrieve a fraction of the pristine properties, analogously to the reduction of graphene oxide.

The choice of purification strategy is primarily determined by two factors: the end use of the nanotubes and the SWCNT type. When selecting a purification route for a particular application, it is important to balance the efficiency of removing metal catalyst and/or non-SWCNT carbons against the damage accumulated in the SWCNTs. For example, SWCNT transistors and other electronic devices require undamaged SWCNTs [25] to maintain high electron mobility, so a mild purification route is preferred. For high surface area SWCNT-based catalyst supports, surface oxidation may be less critical, or even desirable, but metal impurities may need to be excluded rigorously. Different SWCNT synthesis routes lead to differing types and quantities of the impurities in the sample. In addition, the dimensions, crystallinity, chirality, and surface chemistry must be taken into account since they can affect the effectiveness of certain purifications, for example by influencing dissolution kinetics and resistance to oxidation.

Most studies on SWCNT purification concentrate on a particular methodology, often with comparison to a previous related purification technique. As such, the various purification routes in literature are generally performed on different SWCNT types and batches, complicating unambiguous comparisons between the techniques. Here, the effects and efficiencies of possible bulk SWCNT purification routes are compared on a single SWCNT type. Tuball SWCNTs are used as the single SWCNT source, as they are low cost, generally good quality, and available in large volumes, with intermediate impurity levels; independent characterisation of the as-supplied material is provided in this paper.

Seven diverse bulk purification strategies are evaluated in this paper: reflux in hydrochloric acid ('HCl'), reflux in nitric acid ('HNO_3'), treatment with hydrogen peroxide and hydrochloric acid ('H_2O_2/HCl'), oxidation in air at 350 °C ('Air'), oxidisation in nitrogen/steam at 900 °C ('Water vapour'), reduction with sodium naphthalide in DMAc ('NaNp/DMAc'), and electrochemical reduction ('Electrochemical'). The selection of methods includes archetypical examples of key strategies established in the literature, and two recently-developed techniques based on reductive dissolution, all of which in principle may be applicable to the purification of larger quantities of SWNTs. For the present study, 50 mg of raw material was purified in each case for consistency, with the exception of the electrochemical purification, which, as a new method, was limited to 7 mg by the existing equipment. The extent of purification, yield and resultant SWCNT quality between these techniques are systematically compared.

2. Experimental

2.1. Materials and preparation

SWCNTs (Lot # 4-18032014) were purchased from OCSiAl Ltd. Hydrogen peroxide (30% w/w) and hydrochloric acid (37 wt %) were purchased from VWR. Compressed air (21% ±0.5% oxygen, balance nitrogen), oxygen (99.998%) and argon (99.998%) were purchased from BOC Industrial Gasses UK, and all other chemicals were purchased from Sigma Aldrich. Sodium was supplied as ingot (99.95%), naphthalene (99%) was dried *in vacuo* in the presence of P_2O_5. Anhydrous dimethylacetamide (DMAc) and *N*,*N*-dimethylformamide (DMF) were supplied anhydrous and dried over 4 Å and 3 Å molecular sieves respectively, for 2 days prior to use, and sodium perchlorate solutions were dried over 3 Å molecular sieves for 7 days after being mixed. SWCNT reductions were performed in a nitrogen glovebox.

2.2. Purification methods

2.2.1. 'HCl' purification

Raw SWCNT powder (50.0 mg) was refluxed in hydrochloric acid (2 M, 50 mL) for 2 h and filtered over a cellulose membrane (1 μm pore size) and washed with deionised water until the washings reached pH 7. The sample was then dried at 100 °C *in vacuo* overnight to give the purified SWCNTs (46.0 mg). Procedure adapted from Musumeci et al. [26], using a slightly increased HCl concentration (from 1 M) and lower SWCNT scale (from 100 mg); SWCNT concentration was kept the same.

2.2.2. 'H_2O_2/HCl' purification

Raw SWCNT powder (50.0 mg) was stirred in a mixture of 30% hydrogen peroxide solution (30 w/w, 50 mL) and hydrochloric acid (1 M, 50 mL), then heated at 60 °C for 1 h. A further 50 mL of each solution was added after each hour for a total of 4 h. The SWNTs were then filtered over a polytetrafluoroethylene (PTFE) membrane (100 nm pore size) and washed with deionised water until the washings reached pH 7. The sample was then dried at 100 °C *in*

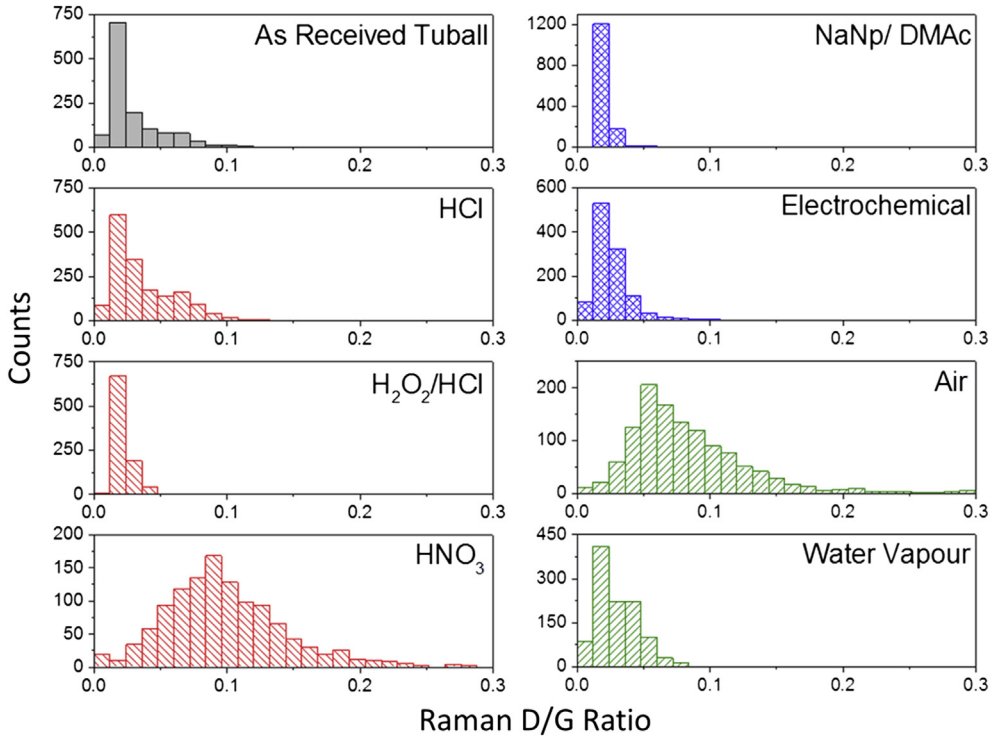

Fig. 1. Normalised histograms of Raman D/G ratios of SWCNT samples before and after purifications. ▩ As-received nanotubes ▨ Acidic purifications ▩ Reductive purifications ▨ Gas phase purifications. N = 910–1672, see ESI Fig. S2. (A colour version of this figure can be viewed online.)

vacuo overnight to give the purified SWCNTs (41.8 mg). Procedure taken from Wang et al. [17].

2.2.3. 'HNO_3' purification

Raw SWCNT powder (50.0 mg) was refluxed in nitric acid (6 M, 36 mL) for 12 h. The liquid turned brown with SWCNTs flocculating in the acid. The solution was filtered over a PTFE membrane (100 nm pore size) and washed with excess NaOH (0.1 M), followed by HCl (0.1 M) until the washings reached pH 7, and finally with excess distilled water. The nanotubes were dried at 100 °C overnight *in vacuo* to give the purified SWCNTs (28.7 mg). Procedure adapted from Hu et al. [27], utilising a higher nitric acid concentration, as preliminary tests using the originally recommended 3 M acid showed poor catalyst removal.

2.2.4. 'Air' purification

Raw SWCNT powder (50.0 mg) was heated from RT to 350 °C at 15 °C min^{-1} under a constant flow of compressed air (100 sccm) and held for 1 h before cooling to RT. The sample was then subjected to the 'HCl purification' as described above to give the purified SWCNTs (19.4 mg). Procedure adapted from Suri et al. [10], using the modified HCl treatment described above, for consistency.

2.2.5. 'Water vapour' purification

Deionised water (200 mL) was deoxygenated by boiling for 1 h and sparging with nitrogen during cooling to RT. Nitrogen (100 sccm) was passed through a bubbler held at 60 °C containing the deoxygenated water and into a furnace containing raw SWCNT powder (50.0 mg). The furnace was heated from RT to 900 °C at 15 °C min^{-1} and held for 3 h before cooling. At 100 °C, the sample was removed from the furnace and subjected to the 'HCl treatment' as described above to give the purified SWCNTs (29.7 mg). Procedure adapted from Tobias et al. [18], with the HCl acid wash added to remove catalyst exposed by the water vapour treatment, as is common in the literature [28]; the SWCNT quantity used was scaled from 400 mg, for consistency.

2.2.6. 'NaNp/DMAc' purification

A bulk solution of sodium naphthalide in DMAc was prepared by stirring sodium (50 mg) and naphthalene (278 mg) in DMAc (50 mL) using a glass stirrer bar. Sodium naphthalide solution (9.6 mL) was diluted to 50 mL and added to raw SWCNT powder (50.0 mg) to give a SWCNT:Na stoichiometry of 10:1, assuming all SWCNT weight is from carbon. The mixture was left overnight unstirred before being centrifuged at 10,000 *g* for 30 min in fluorinated ethylene propylene centrifuge tubes with polytetrafluoroethylene tape sealing the cap thread. The black supernatant was decanted under inert atmosphere and the residual nanotubes were exposed to an atmosphere of dry oxygen for 30 min. The SWCNTs were washed with excess ethanol, water and acetone over a PTFE membrane (100 nm pore size) to give the purified SWCNTs (37.2 mg). Procedure adapted from Clancy et al. [22], using a higher charging ratio, as preliminary tests indicated poor purification at the optimum ratio (20:1) found for Elicarb™ SWCNTs.

2.2.7. 'Electrochemical' purification

Raw SWCNT powder (7 mg) was placed in a custom made four-neck 7 mL cuvette and anhydrous sodium perchlorate solution (DMF, 1 mM, 7 mL) was added. A 100 mm^2 Pt working electrode plate was placed over the SWCNTs and a Pt wire counter electrode and a Ag/Ag^+ reference electrode (0.01 M $AgNO_3$ and 0.1 M tetrabutylammonium perchlorate in acetonitrile, separated by ion permeable frit) were placed in the solution. The working electrode was held at −2.0 V (vs Ag/Ag^+) for 24 h and the solution turned from colourless to black before the solution was decanted. The remaining undissolved SWCNTs were quenched in a dry O_2 environment for 30 min before washing with water and drying at 100 °C overnight to give the purified SWCNTs (5.1 mg). Procedure

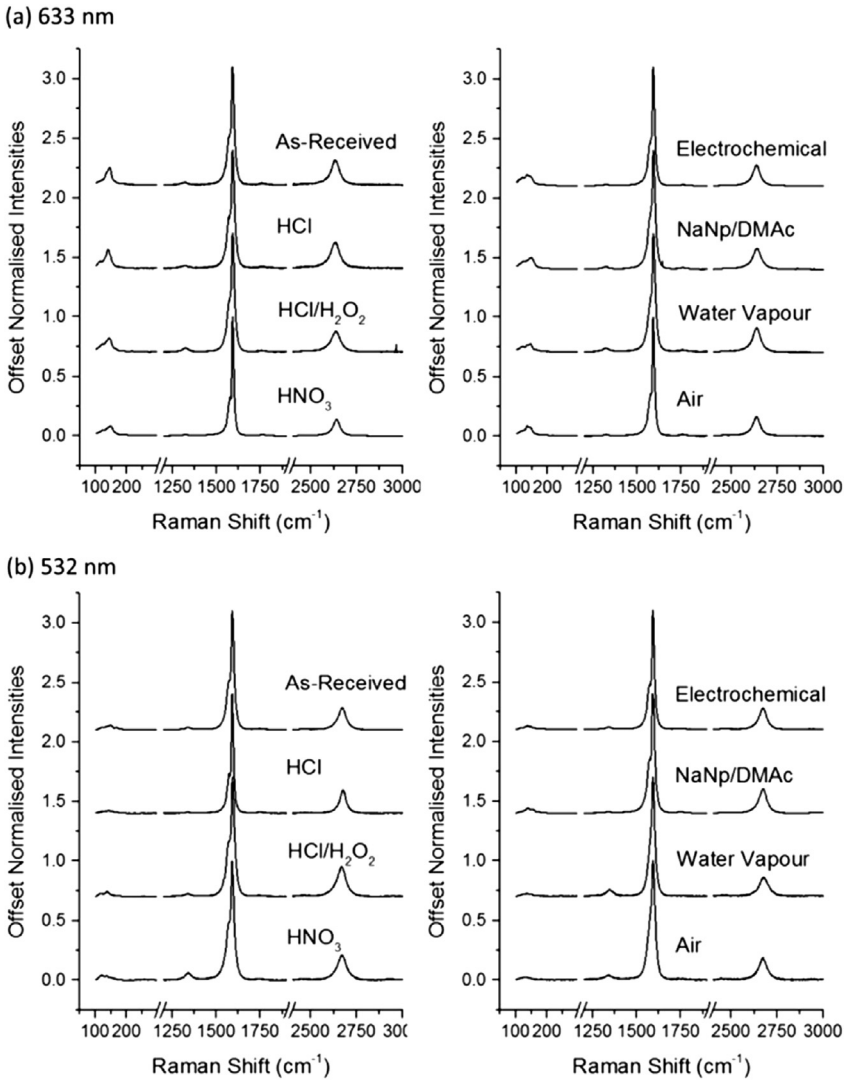

Fig. 2. Full Raman spectra using (a) 633 nm and (b) 532 nm excitation. Average of 10 spectra evenly spaced in a 25 × 125 μm grid.

taken from Hodge et al. [23].

2.3. Characterisation methods

Raman spectroscopy was used to analyse the defectiveness of SWCNT samples by comparing the relative intensities of the D peak (1340 cm^{-1}) and G peak (1589 cm^{-1}). Raman spectroscopy was performed on a Renishaw InVia micro-Raman Spectrometer using a 532 nm (32 mW) or 633 nm (25 mW) laser with 1800 line/mm grating, centred around 2050 cm^{-1} for statistical D/G measurements (Fig. 1). The D/G ratio has high local variance, so was analysed statistically with >1000 spectra per sample using a mapping function over a >200 μm^2 region. Using WiRE 4.1, spectra backgrounds were subtracted ('intelligent fitting', 11th order polynomial, 1.50 noise tolerance) and D, G^-, and G^+ modes were fitted with the Lorentzian function. D/G ratios were calculated using the intensities of D and G^+ peaks. D/G ratios are given using 532 nm excitation due to low intensities of the D peak with 633 nm excitation preventing accurate peak fitting. Complete Raman spectra (Fig. 2) were measured through averaging 10 full spectra (100-3000 cm^{-1}) equally spaced in a 25 × 125 μm array. While there is an inverse relationship between SWCNT defect concentration and 2D mode intensity (ESI, Fig. S1), it is less sensitive to nanotube defects than the D mode [29] and is influenced by other factors such as bundling, strain [30], and doping [31]. Study of the 2D/G ratio is much less common for SWCNTs than MWCNTs or graphenes, and clear changes in intensity are only observed with heavily damage, so analysis here is focussed on D/G ratio.

Thermogravimetric analysis (TGA) gives a qualitative indication of crystallinity of the sample, since defective materials have a lower peak combustion temperature. At temperatures below the combustion temperature, additional weight loss may be seen, associated with amorphous carbon impurities and functional groups. The residual mass can be used to calculate the inorganic impurities (substrate and catalyst); here, the residue is only related to catalyst content as the SWCNTs were not synthesised on a substrate [32]. TGA was performed on a Mettler Toledo TGA/DSC 1. Approximately 2 mg of material was held at 100 °C for 15 min before heating at 10 °C min^{-1} to 850 °C, under air (60 sccm). The temperature of degradation was taken at the temperature with the maximum rate of weight loss; the onset temperature of degradation was not used due to the gradual onset seen for some samples. The initial degradation rate was taken as d (wt%)/d(T) at 300 °C, selected as the temperature at which the rate was linear in all samples, above

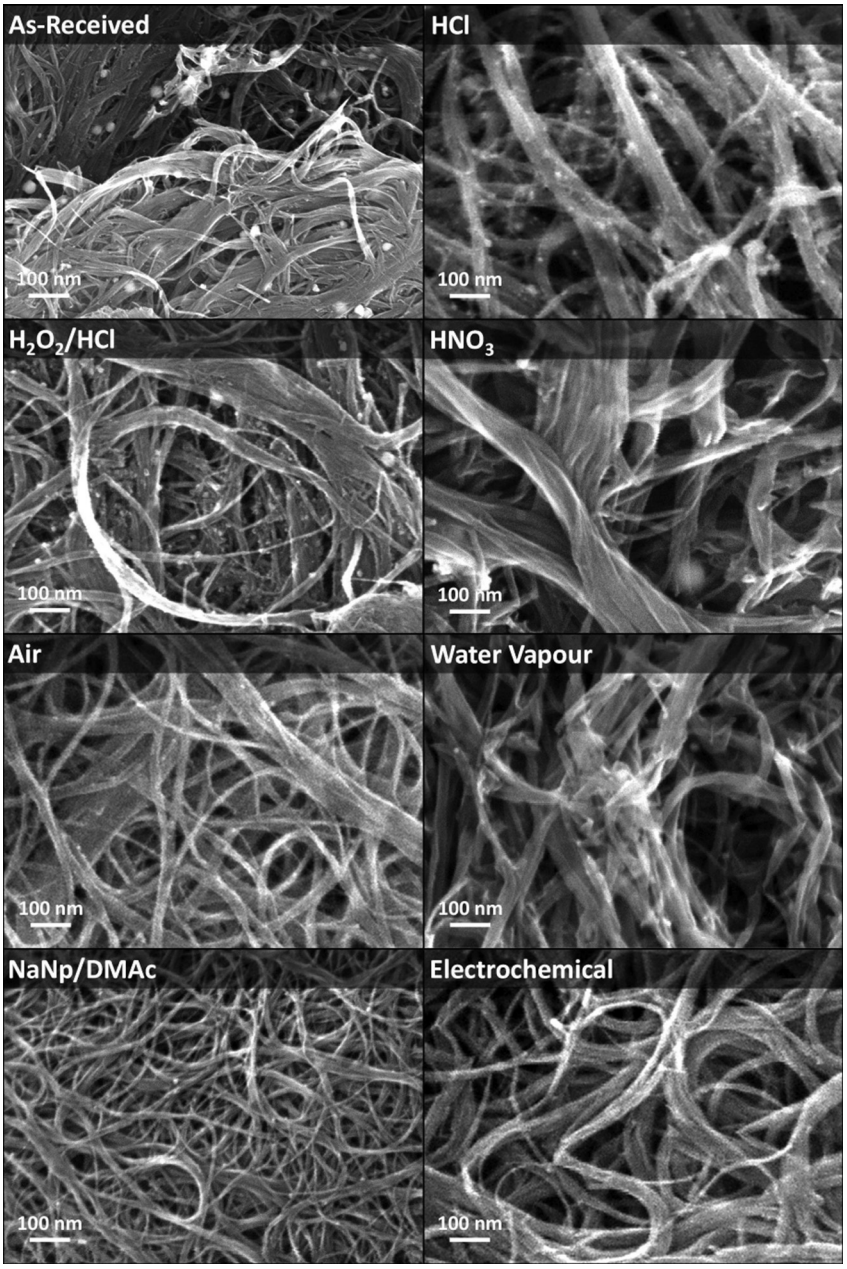

Fig. 3. Typical SEM micrograph of SWCNTs before and after the purification procedures.

temperatures at which weight loss of low volatility solvents may contribute, and below the temperature of bulk SWCNT degradation.

Raw yield was measured from the total weight recovered. Carbon recovery yield was calculated from raw yield in conjunction with the residual weights from TGA of the as-received and purified SWCNTs (Equation 1) to estimate the mass of initial carbon recovered (predominantly SWCNTs, but may include some carbonaceous impurities). For this calculation, it was assumed that all post-TGA residue was Fe_2O_3, originating from metallic iron in the initial samples. Due to the necessary assumptions during this calculation (initial/final iron oxidation states, absence of nickel/iron carbide), both raw mass recovery yield and calculated carbon yield are presented.

$$Y_C = \frac{Y_{Raw}(100 - \varphi W_{ar})}{100 - \varphi W_p}$$

Equation 1. Carbon yield (Y_C), Mass yield (Y_{Raw}), $\varphi = 2M_w\,(Fe)/M_w\,(Fe_2O_3) \approx 0.6994$, weight percentage of inorganic residue in as-received (W_{ar}) and purified (W_p) SWCNTs.

Scanning electron microscopy (SEM) and electron dispersive x-ray spectroscopy (EDX) were performed on a LEO Gemini 1525 FEGSEM at an accelerating voltage of 10 keV for SEM and 20 keV for EDX. Samples were prepared on aluminium stubs and adhered with silver paint. Samples for transmission electron microscopy (TEM) and atomic force microscopy (AFM) were bath sonicated in HPLC ethanol (<1 μg mL^{-1}) and drop-cast onto a holey carbon grid/silicon wafer respectively and dried at RT overnight. Bright field transmission electron microscopy (TEM) was performed on a Jeol 2100FX TEM at 100 keV. AFM measurements were performed by tapping mode on a Digital Instruments Multimode VIII AFM with Nanoscope IV Digital Instruments AFM controller (Veeco) using Nanosensor tapping mode probes (Windsor Scientific). AFM

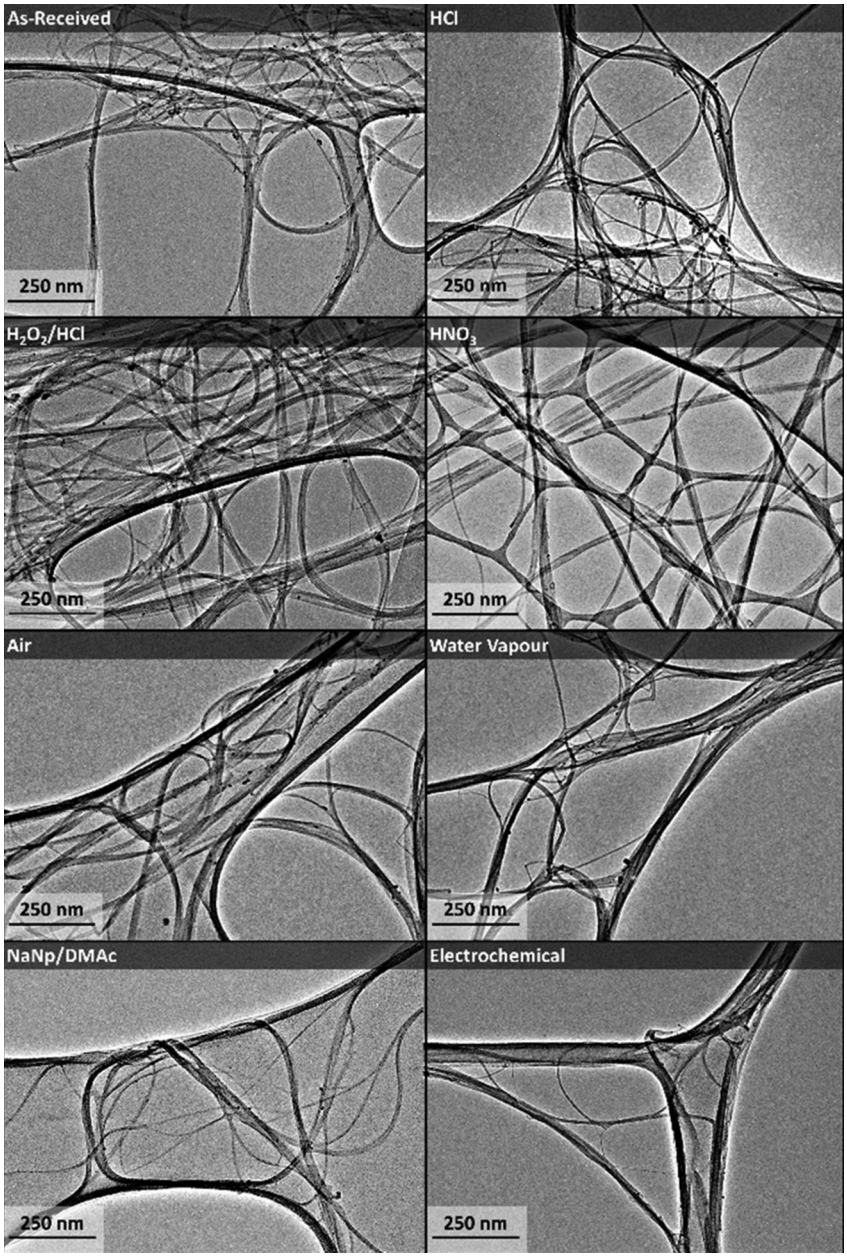

Fig. 4. Typical TEM micrographs of SWCNTs before and after the purification procedures (note that carbon support film is also visible).

micrographs were processed in NanoScope Analysis (v1.40, Bruker), using 3rd order flattening (5% z-threshold) followed by spike removal (3.00).

3. Results and discussion

The as-received SWCNTs can be seen to be relatively long from AFM (1.02^{x}/1.92 μm after sonication and individualisation, ESI, Fig. S3), with diameters between approximately 1.1–2.2 nm (Raman radial breathing modes, ESI Fig. S4). Unfortunately, this distribution is sufficiently wide to preclude the use of NIR/vis spectroscopy as an indicator of sample purity using the NIST method [33], due to an overlap of S_{22} and M_{11} transition energies (ESI Fig. S5). SEM indicates that the raw material consists of macroscopic bundles of SWCNTs, 10–100 nm in diameter, with metal particles on two scales; < 10 nm and ~100 nm (Fig. 3, ESI Fig. S6). EDX (ESI Fig. S7) indicates that the metal is predominantly iron, although a small amount of nickel was found to be present (below the threshold of accurate quantification). TEM supported the presence of metallic impurities while identifying only low levels of amorphous carbon (Fig. 4). Combustion of the as-received SWCNTs had a maximum degradation rate at 644 °C, and left 29.5 wt % inorganic residue (Fig. 5). Statistical Raman spectroscopy (D/G = 0.0310, Fig. 1) showed 46% of spectra with low D/G ratios (≤0.02), with the remaining 54% spread broadly between 0.02 and 0.1 (0.5% > 0.1) forming a tail in the D/G histogram of more defective carbonaceous material (Fig. 1).

3.1. Acidic purifications

After the 'HCl' purification, aside from a slight decrease in inorganic content (24.9 wt %), the bulk material qualities were not

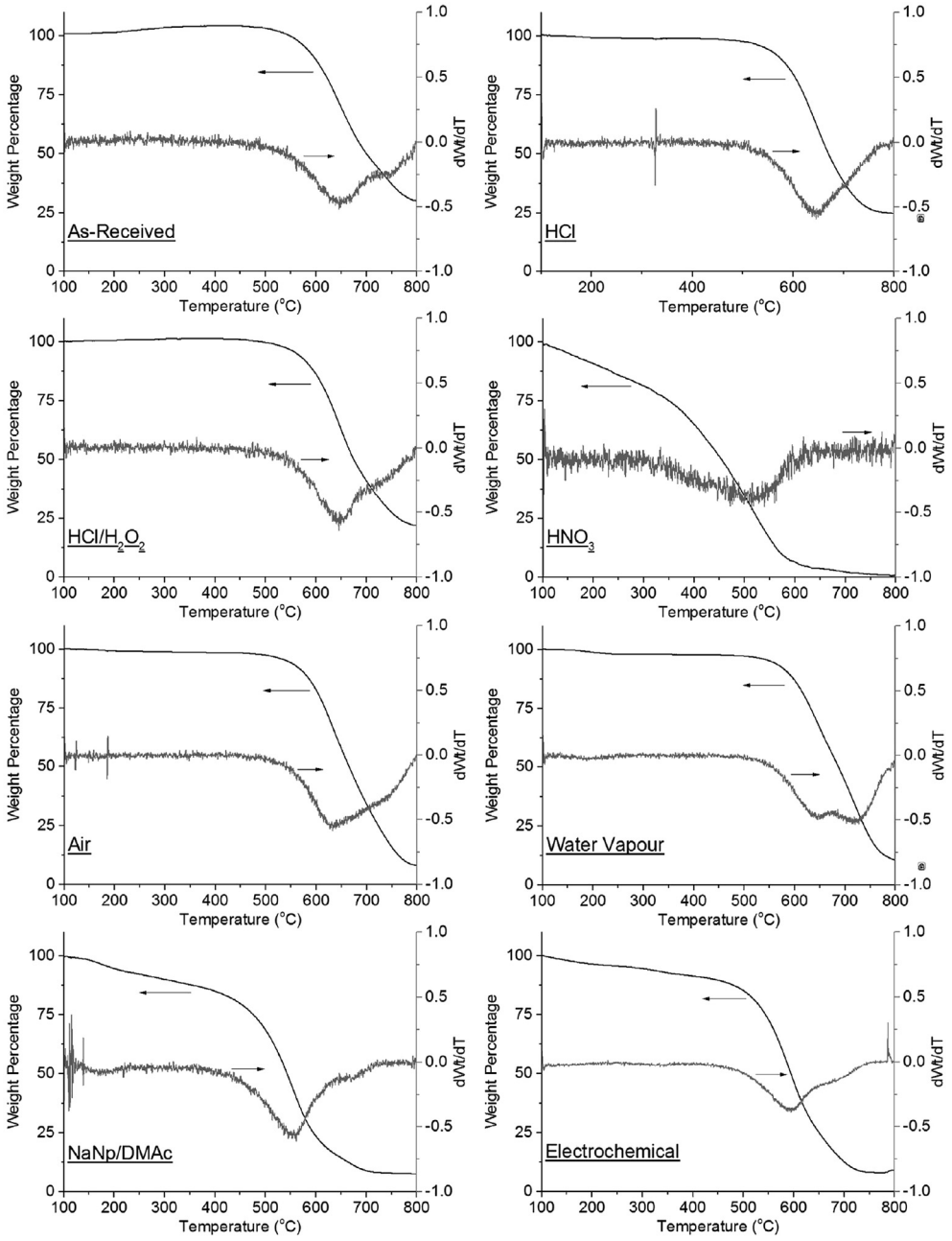

Fig. 5. TGA thermograms (black) and derivatives (grey) of as-received and purified SWCNTs, collected in air.

noticeably altered as the degradation temperature (645 °C) and Raman D/G distribution (D/G = 0.0369) were unaffected after the purification. As expected, these data indicate that the SWCNTs remained intact, but that HCl does not penetrate the carbonaceous encapsulation of the majority of catalytic impurities. 'HCl' purification led to a high recovery of SWCNTs (Fig. 6a, 95.7% carbon yield); the lost carbon is attributed to processing and handling loss rather than reaction, and provides a baseline for other etching reactions.

'H_2O_2/HCl' purification led to a slightly lower inorganic content (21.8 wt %) than HCl treatment, implying some etching of some carbonaceous shells allowing additional catalyst to be removed. The purification also removed some defective material as indicated by the improved D/G ratio (0.0203) although the peak combustion temperature (643 °C) remained unchanged. It is reasonable to suppose that the most defective graphitic shells and possibly some SWCNT end caps were degraded by the hydroxyl radicals from H_2O_2, exposing their internally encapsulated catalyst to the HCl; however, highly graphitic shells (and SWCNT sidewalls) were not significantly attacked. The recovered carbon yield (89.2%) was lower than for pure HCl, consistent with the removal of some carbonaceous materials during the purification.

'HNO_3' purification removed virtually all inorganic impurities (0.1 wt % remaining), however, SWCNT sidewalls were heavily damaged, as seen from the large shift in the average Raman D/G ratio (0.1070) and D/G distribution; 25% of spectra had D/G > 0.125. The damage was further illustrated by the large decrease in peak combustion temperature (508 °C). The early weight loss in TGA from around 200 °C (−0.110 wt % °C^{-1}, Fig. 5) indicates a significant degree of adsorbed organic oxidation debris which can be seen in

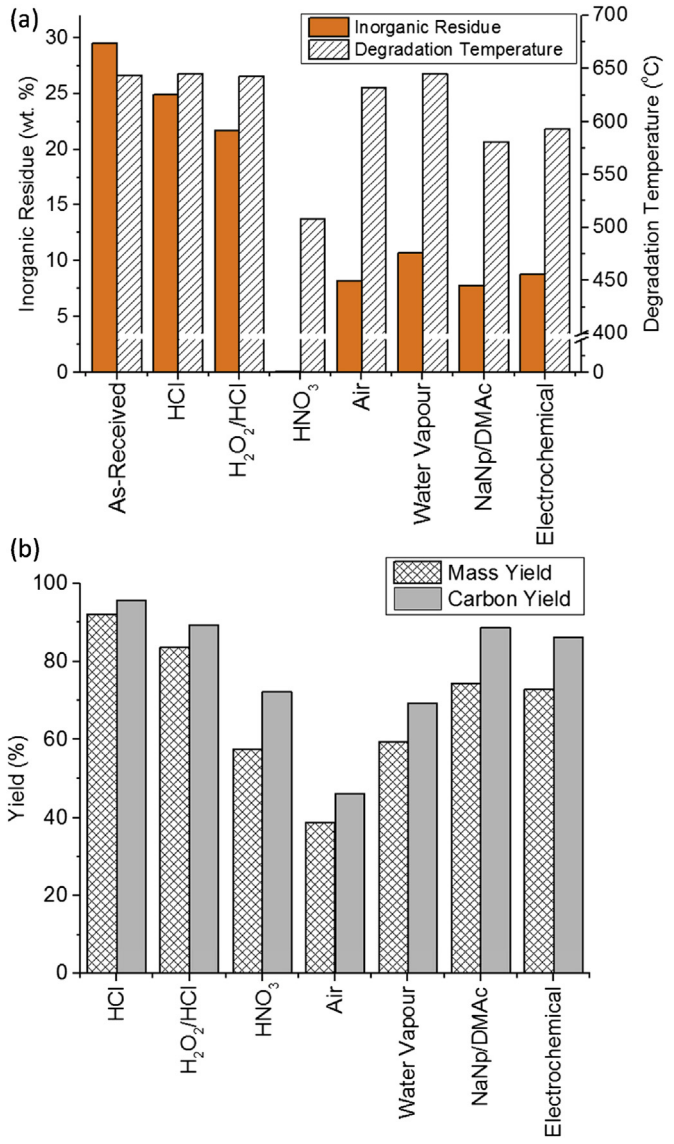

Fig. 6. (a) Inorganic residue (▩) and degradation temperature (▨) of SWCNTs before and after purification procedures. TGAs recorded under air, see Fig. 5 for raw TGA thermograms. Measured inorganic residue will be higher than inorganic impurities in the initial material due to oxidation during the TGA measurement. Initial iron content can be calculated assuming the residue is Fe_2O_3 from Fe^0 (Table 1). (b) Yield of SWCNT purifications; total measured yield (▨) and calculated carbon yield (▩). (A colour version of this figure can be viewed online.)

TEM (Fig. 4), as well as possible surface functionalisation. In addition, the carbon yield of the purification was low (72.2%), indicating that a significant fraction of SWCNTs were destroyed during the purification.

3.2. Gaseous purifications

'Air' purification of SWCNTs led to a significant degree of damage to the SWCNT sample, with a D/G ratio of 0.0908, higher than any route except HNO_3 purification, and the lowest carbon yield (46.0%). The thermal stability was not substantially reduced (632 °C) implying that no significant functionalisation or carbonaceous debris were introduced, consistent with a rate limiting initial oxidation of existing defects or high curvature end caps followed by rapid combustion from the ends [34]. While this cleanliness can be seen as an advantage over 'HNO_3' purification, the catalyst removal (8.2 wt % inorganic residue) was not as efficient.

'Water Vapour' purification was seen to be substantially less damaging to the SWCNT structure than the air purification, with a mild increase in Raman D/G ratio (0.0301) and a similar distribution to the as-received material. The combustion temperature (645 °C) was likewise unaltered and the carbon yield (69.2%) was notably higher than the 'Air' purification, complementing the lack of damage incurred during the purification. However, catalyst removal was not particularly effective, with 10.7 wt % inorganic residue remaining.

3.3. Reductive purifications

'NaNp/DMAc' purification removed a significant proportion of catalyst (29.5 wt % inorganic TGA residue reduced to 7.8 wt % remaining), superior to all but the nitric acid purification. The temperature of maximum combustion decreased to 581 °C which may be attributed to the large degree of debundling (Fig. 3) that is typically seen in these reductive systems [35]. Some weight loss was seen below the temperature of combustion implying modest functionalisation during charge quenching, however, the notable decrease in D/G ratio in the Raman spectra (0.020) suggests that only a small degree of functionalisation was introduced. The modal D/G ratio remains unchanged implying little structural change to the remaining SWCNTs. A high carbon yield of 88.6% was obtained for this purification procedure.

'Electrochemical' purification of SWCNTs was similar to 'NaNp/DMAc' purification, in spite of the difference in scale, with regards to catalyst removal (8.8 wt % remaining residue), damage to the SWCNT structure (D/G = 0.0280), and carbon yield (86.2%). The resultant purified material did not show debundling to the same

Table 1
Table of properties of SWCNTs before and after purifications. D/G ratio from Raman spectra (standard deviations and *N* are available in ESI, Fig. S2). T_{degrad} taken at temperature with highest derivative of mass loss per degree (Fig. 5). Initial degradation rate taken as rate of weight loss at 300 °C, *i.e.* prior to SWCNT combustion, after solvent removal. Inorganic content taken as percentage weight of material at 800 °C, after SWCNT combustion in TGA. Iron content is calculated from inorganic residue, assuming all inorganic residue is a product of the oxidation of metallic iron to iron (III) oxide. Mass yield given as weight of material recovered as a percentage of mass of SWCNTs purified, carbon yield calculated according to Equation 1.

Purification route		Raman (D/G)	T_{degrad} (°C)	Initial Deg. Rate (wt %/°C)	Inorganic TGA residue (wt %)	Calc. Initial Fe content (wt %)	Yield (%)	
							Mass	Carbon
None (As-received)		0.0310	644	0.025	29.5	20.6	–	–
Acidic	HCl	0.0369	645	0.004	24.9	17.4	92.0	95.7
	HNO_3	0.1070	508	−0.110	0.10	0.07	83.6	89.3
	H_2O_2/HCl	0.0203	643	0.014	21.8	15.2	57.4	72.2
Gaseous	Air	0.0908	632	−0.002	8.2	5.74	38.8	46.1
	Water Vapour	0.0301	645	0.001	10.7	7.48	59.4	69.2
Reductive	NaNp/DMAc	0.0202	581	−0.007	7.8	5.45	74.4	88.6
	Electrochemical	0.0280	593	−0.011	8.8	6.12	72.9	86.2

extent as the NaNp/DMAc purification route (Fig. 3), which is thought to be due to the pressure of the platinum electrode (required to permit charge transfer) limiting swelling. The more heavily bundled SWCNTs subsequently showed a higher degradation temperature than the NaNp/DMAc route (593 °C).

3.4. Comparison of purifications

As noted earlier, the ideal purification procedure is fundamentally dependent on the desired application of the resulting SWCNTs. The reductive purifications and 'Water Vapour' purification remove a majority of impurities with minimal SWCNT damage. The reductive purifications are similar in most regards, but in most chemistry laboratories the NaNp/DMAc purification will be simpler to implement. The electrochemical approach requires more specialist equipment, is currently small scale, and relatively time consuming. However, for possible future industrial scale-up, these issues may be mitigated and the electrochemical approach could offer advantages, particularly avoiding the use of sodium metal. It is worth noting that industrial-scale electrochemical purification of conventional metals is well established, including in inert atmospheres. The yield and impurity removal of 'NaNp/DMAc' is superior to 'Water Vapour' while giving similar degrees of functionalisation, as judged by Raman spectroscopy, suggesting that NaNp/DMAc may be the best route. On the other hand, TGA does indicate some degree of damage introduced using the reductive routes, which may be mitigated by different approaches to charge quenching [22], or alternatively, the charge may be exploited to introduce desired functional groups deliberately [36].

'Air' purification is commonly employed as a compromise purification, however, the higher defectiveness of the SWCNTs and lower yield compared to NaNp/DMAc leads to the conclusion that 'Air' purification should generally be avoided for these particular SWCNTs. In situations where iron removal is a priority, 'HNO_3' purification is the best purification route as it eliminates all inorganic residue measurable by TGA, however, it also causes a significant degree of SWCNT sidewall damage. Conversely, when the removal of inorganic impurities is of lesser importance than the retention of the SWCNT sp^2 framework, 'NaNp/DMAc' should be selected. While the 'H_2O_2/HCl' purification led to similar levels of defectiveness as illustrated by D/G mode intensities, it was less efficient at impurity removal than NaNp/DMAc. However, some researchers may find the 'H_2O_2/HCl' purification route useful, owing to its speed and ease of implementation. While 'HCl' purification also preserves the SWCNT structure, it does so with a significantly inferior degree of impurity removal and is not recommended.

4. Conclusion

This study provides a broad comparison of SWCNT purification routes with consistency in SWCNT type and batch. The routes described do not involve any ultrasonication or ultracentrifugation, and therefore in principle should be scalable to larger quantities, with appropriate mixing conditions, and precautions for the aggressive reagents. There is currently no single ideal purification process for SWCNTs; the choice of purification route is strongly dependent on the desired properties of the final product. The new 'NaNp/DMAc' purification offers the best compromise of impurity removal without sacrificing SWCNT yield and structural integrity. 'Water Vapour' purification is a suitable alternative without requiring the potentially restrictive inert conditions, at the cost of diminished yield and inferior catalyst removal. In scenarios where catalyst removal is critical, traditional 'HNO_3' purification can be performed, although yield and SWCNT framework are heavily compromised. While these trends have been measured for Tuball™ SWCNTs, they are expected to be broadly consistent across a range of SWCNT types. Further optimisation of the purification conditions will likely allow quantitatively superior results to be obtained, although the qualitative trends are not expected to alter dramatically; the findings of this study should allow future work on functionalisation to be directed effectively.

Acknowledgements

The authors would like to thank the EPSRC (Program Grant EP/I02946X/1 on high performance ductile composite technology in collaboration with Bristol University, and EP/L001896/1 on electrochemical processing of discrete nanoparticle ions) and Thomas Swan Ltd., as well as the FP7 Project MATFLEXEND (# 604093), for funding this work. H.H.T. thanks the National Research Foundation, Energy Innovations Programme Office, Singapore.

Appendix A. Supplementary data

Supplementary data related to this article can be found at http://dx.doi.org/10.1016/j.carbon.2016.07.034.

References

[1] J. Coleman, U. Khan, W. Blau, Y. Gun'ko, Small but strong: a review of the mechanical properties of carbon nanotube–polymer composites, Carbon 44 (2006) 1624–1652, http://dx.doi.org/10.1016/j.carbon.2006.02.038.
[2] S.A. Hodge, Mustafa K. Bayazit, Karl S. Coleman, M.S.P. Shaffer, Unweaving the rainbow: a review of the relationship between single-walled carbon nanotube molecular structures and their chemical reactivity, Chem. Soc. Rev. 41 (2012) 4409–4429, http://dx.doi.org/10.1039/c2cs15334c.
[3] P. Avouris, Z. Chen, V. Perebeinos, Carbon-based electronics, Nat. Nanotechnol. 2 (2007) 605–615, http://dx.doi.org/10.1038/nnano.2007.300.
[4] H. Zhu, B. Wei, Assembly and applications of carbon nanotube thin films, J. Mater. Sci. Technol. 24 (2008) 447–456.
[5] A. Bianco, K. Kostarelos, M. Prato, Applications of carbon nanotubes in drug delivery, Curr. Opin. Chem. Bio. 9 (2005) 674–679, http://dx.doi.org/10.1016/j.cbpa.2005.10.005.
[6] P.-X. Hou, C. Liu, H.-M. Cheng, Purification of carbon nanotubes, Carbon 46 (2008) 2003–2025, http://dx.doi.org/10.1016/j.carbon.2008.09.009.
[7] T.-J. Park, S. Banerjee, T. Hemraj-Benny, S. Wong, Purification strategies and purity visualization techniques for single-walled carbon nanotubes, J. Mater. Chem. 16 (2006) 141–154, http://dx.doi.org/10.1039/b510858f.
[8] X. Huang, R.S. McLean, M. Zheng, High-resolution length sorting and purification of DNA-wrapped carbon nanotubes by size-exclusion chromatography, Anal. Chem. 77 (2005) 6225–6228, http://dx.doi.org/10.1021/ac0508954.
[9] Y. Matsuzawa, Y. Takada, T. Kodaira, H. Kihara, H. Kataura, M. Yoshida, Effective nondestructive purification of single-walled carbon nanotubes based on high-speed centrifugation with a photochemically removable dispersant, J. Phys. Chem. C 118 (2014), http://dx.doi.org/10.1021/jp411964z.
[10] A. Suri, K.S. Coleman, The superiority of air oxidation over liquid-phase oxidative treatment in the purification of carbon nanotubes, Carbon 49 (2011) 3031–3038, http://dx.doi.org/10.1016/j.carbon.2011.03.023.
[11] H. Hu, B. Zhao, M.E. Itkis, R.C. Haddon, Nitric acid purification of single-walled carbon nanotubes, J. Phys. Chem. B 107 (2003) 13838–13842, http://dx.doi.org/10.1021/jp035719i.
[12] T. Sun, T. Zeng, C. Xia, S. Li, H. Wu, Purification and separation of single-walled carbon nanotubes, J. Nanosci. Nanotechnol. 12 (2012) 2955–2963, http://dx.doi.org/10.1166/jnn.2012.5741.
[13] R. Verdejo, S. Lamoriniere, B. Cottam, A. Bismarck, M. Shaffer, Removal of oxidation debris from multi-walled carbon nanotubes, Chem. Commun. (2007) 513–515.
[14] J.P. Rourke, P.A. Pandey, J.J. Moore, M. Bates, I.A. Kinloch, R.J. Young, et al., The real graphene oxide revealed: stripping the oxidative debris from the graphene like sheets, Angew. Chem. 123 (2011) 3231–3235, http://dx.doi.org/10.1002/anie.201007520.
[15] Y. Li, X. Zhang, J. Luo, W. Huang, J. Cheng, Z. Luo, Purification of CVD synthesized single-wall carbon nanotubes by different acid oxidation treatments, Nanotechnology 15 (1645) (2004), http://dx.doi.org/10.1088/0957-4484/15/11/047.
[16] T.J. Aitchison, M. Ginic-Markovic, Purification, cutting, and sidewall functionalization of multiwalled carbon nanotubes using potassium permanganate solutions, J. Phys. Chem. C 111 (2007) 2440–2446, http://dx.doi.org/10.1021/jp066541d.
[17] Y. Wang, H. Shan, R.H. Hauge, M. Pasquali, R.E. Smalley, A highly selective, one-pot purification method for single-walled carbon nanotubes, J. Phys.

Chem. B 111 (2007) 1249–1252, http://dx.doi.org/10.1021/jp068229+.
[18] G. Tobias, L. Shao, C.G. Salzmann, Y. Huh, M.L. Green, Purification and opening of carbon nanotubes using steam, J. Phys. Chem. B 110 (2006) 22318–22322, http://dx.doi.org/10.1021/jp0631883.
[19] A. Pénicaud, P. Poulin, A. Derré, E. Anglaret, P. Petit, Spontaneous dissolution of a single-wall carbon nanotube salt, J. Am. Chem. Soc. 127 (2005) 8–9, http://dx.doi.org/10.1021/ja0443373.
[20] D. Voiry, C. Drummond, A. Pénicaud, Portrait of carbon nanotube salts as soluble polyelectrolytes, Soft Matt. 7 (2011) 7998–8001, http://dx.doi.org/10.1039/c1sm05959a.
[21] S. Fogden, C.A. Howard, R.K. Heenan, N.T. Skipper, M.S. Shaffer, Scalable method for the reductive dissolution, purification, and separation of single-walled carbon nanotubes, ACS nano 6 (2012) 54–62, http://dx.doi.org/10.1021/nn2041494.
[22] A.J. Clancy, J. Melbourne, M.S.P. Shaffer, A one step route to solubilised, purified or functionalised single-walled carbon nanotubes, J. Mater. Chem. A 3 (2015) 16708–16715, http://dx.doi.org/10.1039/C5TA03561A.
[23] S.A. Hodge, S. Fogden, C.A. Howard, N.T. Skipper, M.S.P. Shaffer, Electrochemical processing of discrete single-walled carbon nanotube anions, ACS nano 7 (2013) 1769–1778, http://dx.doi.org/10.1021/nn305919p.
[24] B. Gebhardt, F. Hof, C. Backes, M. Müller, T. Plocke, J. Maultzsch, et al., Selective polycarboxylation of semiconducting single-walled carbon nanotubes by reductive sidewall functionalization, J. Am. Chem. Soc. 133 (2011) 19459–19473, http://dx.doi.org/10.1021/ja206818n.
[25] B. King, B. Panchapakesan, Vacuum filtration based formation of liquid crystal films of semiconducting carbon nanotubes and high performance transistor devices, Nanotechnology 25 (175201) (2014), http://dx.doi.org/10.1088/0957-4484/25/17/175201.
[26] A.W. Musumeci, E.R. Waclawik, R.L. Frost, A comparative study of single-walled carbon nanotube purification techniques using Raman spectroscopy, Spectrochim. Acta Mol. Biomol. Spectrosc. 71 (2008) 140–142, http://dx.doi.org/10.1016/j.saa.2007.11.019.
[27] H. Hu, B. Zhao, M.E. Itkis, R.C. Haddon, Nitric acid purification of single-walled carbon nanotubes, J. Phys. Chem. B 107 (2003) 13838–13842, http://dx.doi.org/10.1021/jp035719i.
[28] A.F. Holloway, K. Toghill, G.G. Wildgoose, R.G. Compton, M.A.H. Ward, G. Tobias, et al., Electrochemical opening of single-walled carbon nanotubes filled with metal halides and with closed ends, J. Phys. Chem. C 112 (2008) 10389–10397, http://dx.doi.org/10.1021/jp802127p.
[29] Dresselhaus, G. Dresselhaus, R. Saito, A. Jorio, Raman spectroscopy of carbon nanotubes, Phys. Rep. 409 (2005), http://dx.doi.org/10.1016/j.physrep.2004.10.006.
[30] M.S. Dresselhaus, A. Jorio, M. Hofmann, G. Dresselhaus, R. Saito, Perspectives on carbon nanotubes and graphene raman spectroscopy, Nano Lett. 10 (2010) 751–758, http://dx.doi.org/10.1021/nl904286r.
[31] M.V. Kharlamova, Advances in tailoring the electronic properties of single-walled carbon nanotubes, Prog. Mater. Sci. 77 (2016) 125–211, http://dx.doi.org/10.1016/j.pmatsci.2015.09.001.
[32] M. R. Baptist, Patent number RU 2157060, ПлазМохиМический реактор..
[33] S. Freiman, Measurement Issues in Single Wall Carbon Nanotubes, (NIST Special Publication), 2008.
[34] Y. Miyata, T. Kawai, Y. Miyamoto, K. Yanagi, Y. Maniwa, H. Kataura, Chirality-dependent combustion of single-walled carbon nanotubes, J. Phys. Chem. C 111 (2007) 9671–9677, http://dx.doi.org/10.1021/jp072359g.
[35] A. Pénicaud, F. Dragin, G. Pécastaings, M. He, E. Anglaret, Concentrated solutions of individualized single walled carbon nanotubes, Carbon 67 (2014) 360–367, http://dx.doi.org/10.1016/j.carbon.2013.10.006.
[36] F. Hof, S. Bosch, S. Eigler, F. Hauke, A. Hirsch, New basic insight into reductive functionalization sequences of single walled carbon nanotubes, J. Am. Chem. Soc. 135 (2013) 18385–18395, http://dx.doi.org/10.1021/ja4063713.